

## Predicted power laws for delayed switching of charge-density waves

Steven H. Strogatz\* and Robert M. Westervelt

*Division of Applied Sciences and Department of Physics, Harvard University, Cambridge, Massachusetts 02138*

(Received 15 May 1989)

We analyze delayed conduction in three recent models of switching charge-density waves. Each model predicts a power-law dependence of switching delay near threshold:  $\tau \sim \epsilon^{-\beta}$ , where  $\tau$  is the delay and  $\epsilon \equiv (E - E_T)/E_T$  is the normalized distance above the threshold field  $E_T$ . Using bifurcation theory, we show that the models of Hall *et al.* and Mihaly *et al.* predict  $\tau \sim \epsilon^{-1/2}$ , whereas the model of Strogatz *et al.* predicts  $\tau \sim \epsilon^{-1}$ . These different predictions allow the models to be distinguished experimentally.

### I. INTRODUCTION

There is a great deal of experimental and theoretical interest in charge-density-wave (CDW) transport.<sup>1,2</sup> It has been shown experimentally that CDW conduction occurs only if the local electric field  $E$  exceeds a depinning threshold  $E_T$ . For fields below the depinning threshold, the CDW is pinned to the lattice by impurities and other defects. For  $E > E_T$  the CDW breaks free from the pinning sites and begins to slide and carry current. Much of the work on CDW transport has focused on CDW's which depin smoothly as the applied field is increased.<sup>3-6</sup> These systems are characterized by continuous and nonhysteretic current-voltage characteristics.

In 1982, Zetzl and Grüner<sup>7</sup> described a novel form of CDW transport in NbSe<sub>3</sub> in which the system "switches" discontinuously and hysteretically between the pinned and sliding states. Switching has since been studied in other CDW materials<sup>8-10</sup> as well as in NbSe<sub>3</sub>,<sup>11-14</sup> and a number of theoretical models for switching have been proposed recently.<sup>15-23</sup>

One of the most intriguing phenomena associated with switching is a delayed onset of CDW conduction close to threshold.<sup>7-9,11</sup> In response to a suddenly applied electric field above the depinning threshold, the CDW does not depin immediately—there is a time delay before the CDW begins to slide. This delay can range over several orders of magnitude, from about 0.1 to 1000 microseconds.<sup>7-9,11</sup>

Similar delayed transitions occur in a wide variety of driven dynamical systems. Examples include delayed phase transitions in ferroelectrics,<sup>24</sup> hangup in phase-locked loops,<sup>25</sup> delayed firing in neurons,<sup>26</sup> and turn-on delay in semiconductor lasers<sup>27</sup> and Josephson junctions.<sup>28,29</sup>

For the case of CDW's, an important open question is the dependence of the switching delay  $\tau$  on the normalized overdrive  $\epsilon \equiv (E - E_T)/E_T$ . It has been shown experimentally that the delay increases as threshold is approached from above,<sup>8,9</sup> but the functional dependence of  $\tau$  on  $\epsilon$  remains to be clarified. This functional dependence would provide a benchmark for distinguishing

among the different models of CDW switching.

In Sec. II we analyze three recent models of switching, and show that they all predict a power-law dependence of the switching delay  $\tau$  on the overdrive  $\epsilon$ . Close to threshold, the amplitude-collapse model<sup>16,17</sup> and the screening model<sup>18</sup> both predict  $\tau \sim \epsilon^{-1/2}$ , whereas the mean-field phase-slip model<sup>19-21</sup> predicts  $\tau \sim \epsilon^{-1}$ . These power laws are obtained by bifurcation analysis of the depinning transition in each of the models. We show that numerical results agree with the predictions from bifurcation theory, and we present phase-plane analyses which allow one to visualize the "bottlenecks" underlying the delay in the models. Section III offers concluding remarks and discusses possible experimental tests of the predicted power laws.

### II. ANALYSIS OF MODELS

#### A. Amplitude-collapse model

Hall *et al.*<sup>16</sup> and Inui *et al.*<sup>17</sup> have presented a model of CDW switching based on the ideas of phase polarization, amplitude collapse, and phase slip between strongly pinned CDW domains. We review the physical ideas behind the model and then present its governing equations.

In the amplitude-collapse model, switching samples are imagined to be composed of weakly pinned bulk regions and strongly pinned domains. The effect of an applied field above the bulk threshold is to polarize the CDW about its strongly pinned regions. As the field is increased the strongly pinned domains are not dislodged; instead the elastic cost of the additional polarization drives the CDW amplitude toward zero.

Hall *et al.*<sup>16</sup> and Inui *et al.*<sup>17</sup> hypothesize that as the amplitude decreases, the phase elasticity weakens. This sets up positive feedback with polarization increasing and amplitude decreasing until the amplitude is ultimately driven to zero. At the moment of amplitude collapse, a  $2\pi$  phase slip occurs and relieves the polarization, paving the way for another round of polarization buildup and amplitude collapse. If the amplitude recovers insufficiently before the next collapse, a switch to the sliding state may be triggered.

These ideas have been formalized in the following system of equations:<sup>16,17</sup>

$$\frac{d\phi}{dt} = E - \sin\phi - \alpha\Delta(\phi - \phi_0), \quad (1a)$$

$$\frac{d\Delta}{dt} = \frac{1}{\kappa} \left[ 1 - \Delta - \left[ \frac{\phi - \phi_0}{\theta} \right]^2 \right], \quad (1b)$$

$$\phi_0 \rightarrow \begin{cases} \phi_0 + 2\pi \operatorname{sgn}(\phi - \phi_0) & \text{if } \Delta = 0 \\ \phi_0 & \text{if } \Delta \neq 0. \end{cases} \quad (1c)$$

For simplicity only two domains are involved in Eq. (1), one strongly pinned and one weakly pinned. In Eq. (1),  $\phi$  is the phase of a weakly pinned bulk region,  $\phi_0$  is the phase of a strongly pinned domain, and  $\Delta$  is the CDW amplitude at the strong pinning center. The parameters have the following interpretation:  $E$  is proportional to the applied electric field;  $\theta$  determines how much polarization can be built up before phase slip occurs;  $\alpha$  is the stiffness of the phase mode; and  $\kappa$  is the ratio of phase to amplitude relaxation rates.

To see how delayed switching occurs in Eq. (1), it is helpful to visualize the flow in phase space. Figure 1(a)

shows the  $(\phi, \Delta)$  phase plane just below the depinning threshold. There are two equilibrium points: a stable node and a saddle point nearby. The stable node corresponds to a pinned state with a large polarization. The proximity of the saddle point to the stable node indicates that the system is on the verge of phase slip. As  $E$  is increased toward the depinning threshold  $E_T$ , the saddle and node approach each other and ultimately coalesce at  $E = E_T$ .

Figure 1(b) plots the phase plane *after* the depinning transition. There is a bottleneck region of phase space, a “ghost” of the former saddle node where the dynamics are slow. Trajectories are funneled into the bottleneck [Fig. 1(b)], and spend a long time passing through there. The time spent in the bottleneck scales as  $\varepsilon^{-1/2}$ , where  $\varepsilon \equiv (E - E_T)/E_T$ . This square-root scaling law holds *generically* for systems in the aftermath of a saddle-node bifurcation (see Ref. 30, p. 344). For example, the same scaling law arises in analyses of type-I intermittency<sup>31</sup> and turn-on delay in overdamped Josephson logic circuits.<sup>29</sup> Close to threshold ( $\varepsilon \rightarrow 0$ ), the time spent passing through the bottleneck dominates all other time scales in the problem, and therefore gives a good approximation to the total delay.

To test the square-root scaling expected from bifurcation theory, we integrated Eq. (1) numerically, starting from the zero-field pinned state  $\Delta = 1, \phi = 0$ . This initial condition corresponds to experiments on delayed switching, where the system is first allowed to relax in zero field.<sup>7-9,11</sup> At  $t = 0$  the field  $E$  is turned on. Figure 2 shows the evolution of the amplitude for two different values of applied field. The switching delay increases as  $E$  approaches  $E_T$ . To make this statement more quantitative, we define the delay  $\tau$  as the time required for the

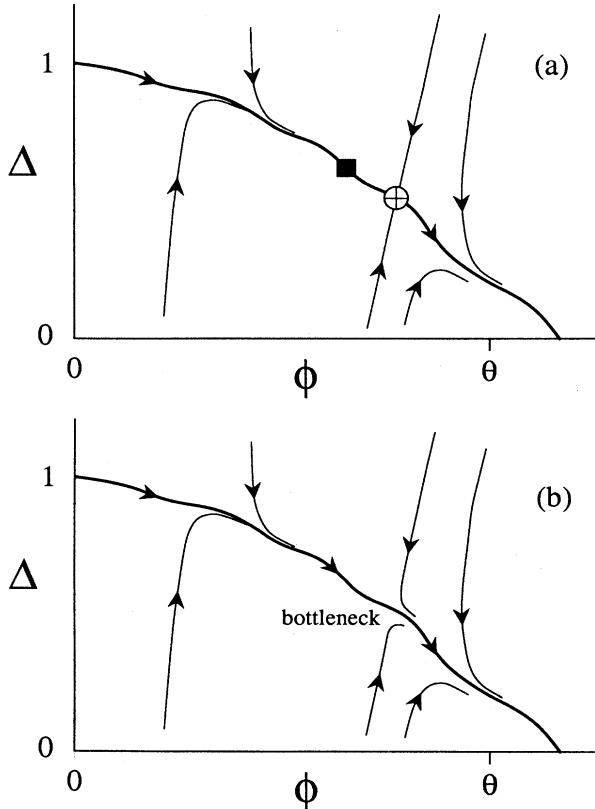


FIG. 1. Phase plane for the amplitude-collapse model Eq. (1). Parameters:  $\alpha = 0.2, \kappa = 0.7, \theta = 10\pi, \phi_0 = 0$ , as used in Ref. 17. For these parameters the depinning threshold is  $E_T \approx 3.36$ . (a) For  $E = 3.3$ , there are two equilibria: a stable node (solid square) and a saddle point (crossed circle). (b) For  $E = 3.4$ , the saddle and node have coalesced, leaving a remnant “bottleneck” into which trajectories are funneled. Time delay is caused by the slow passage of trajectories through this bottleneck.

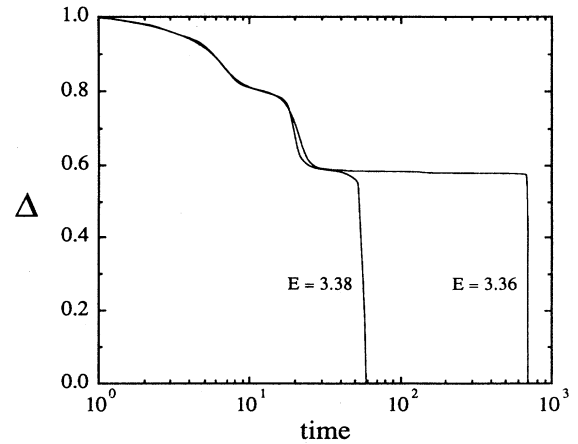


FIG. 2. Delayed collapse of the dimensionless amplitude  $\Delta$  in Eq. (1), for two values of  $E$  above the depinning threshold. Note that the time axis is logarithmic and dimensionless. Solutions obtained by numerical integration of Eq. (1), with  $E = 3.36$  and  $3.38$  and initial conditions  $\Delta = 1, \phi = 0$ ; other parameters as in Fig. 1. As  $E$  approaches the depinning threshold ( $E_T \approx 3.359947$ ), there is an increasing time delay before the amplitude collapses.

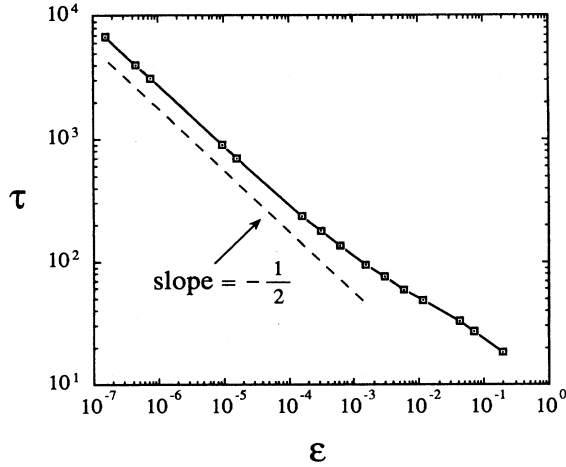


FIG. 3. Dependence of delay  $\tau$  on overdrive  $\varepsilon \equiv (E - E_T)/E_T$ , for the amplitude-collapse model Eq. (1). Parameters as in Fig. 1. Both  $\tau$  and  $\varepsilon$  are dimensionless. For small  $\varepsilon$  the curve has a slope of  $-\frac{1}{2}$ , in agreement with bifurcation theory.

CDW amplitude to collapse for the first time. This delay is found by integrating the equations numerically until  $\Delta=0$ .

Figure 3 shows that very close to threshold the delay scales as  $\varepsilon^{-1/2}$ . However, for values of  $\varepsilon$  larger than about  $10^{-3}$  the curve becomes more shallow with a slope between  $-\frac{1}{2}$  and 0.

### B. Screening model

The physical idea of the screening model proposed by Mihaly, Chen, and Grüner<sup>18</sup> is that deformations of the CDW lead to local charge fluctuations which are screened by conduction electrons not condensed into the CDW. The screening currents introduce Ohmic dissipation which damps the relative motion of CDW domains.

The equations for the model are

$$\frac{d\Phi_1}{dt} + \gamma \left[ \frac{d\Phi_1}{dt} - \frac{d\Phi_2}{dt} \right] + K(\Phi_1 - \Phi_2) = E + \sin\Phi_1, \quad (2a)$$

$$\frac{d\Phi_2}{dt} + \gamma \left[ \frac{d\Phi_2}{dt} - \frac{d\Phi_1}{dt} \right] + K(\Phi_2 - \Phi_1) = E - \sin\Phi_2, \quad (2b)$$

where  $\Phi_1$  and  $\Phi_2$  are the phases of two coupled domains,  $\gamma$  is the viscous coupling strength,  $K$  is the elastic coupling strength, and  $E$  is proportional to the applied electric field. The viscous term reflects the internal damping due to the screening effects of the normal electrons. The pinning strength has been normalized to one in the  $\sin\Phi$  terms.

It is convenient to rewrite Eq. (2) in terms of new variables  $\phi$  and  $\psi$ , defined as  $\phi = (\Phi_1 - \Phi_2)/2$  and  $\psi = (\Phi_1 + \Phi_2)/2$ . This yields

$$\frac{d\psi}{dt} = E + \frac{1}{2}[\sin(\psi + \phi) + \sin(\psi - \phi)], \quad (3a)$$

$$\frac{d\phi}{dt} = \frac{1}{1 + 2\gamma} \left\{ -2K\phi + \frac{1}{2}[\sin(\psi + \phi) + \sin(\psi - \phi)] \right\}. \quad (3b)$$

For this model the current carried by the CDW is proportional to  $d\psi/dt$ .

Figure 4(a) shows the phase plane for Eq. (3) just below the depinning threshold. There is a stable node corresponding to the pinned state, and a saddle point close to it. As in the amplitude-collapse model, the depinning transition in the screening model occurs via a saddle-node bifurcation in phase space. As  $E$  is increased, the saddle and the node approach each other and coalesce at  $E = E_T$ . Note that there is also a stable limit cycle in Fig. 4(a)—it corresponds to the sliding state of the CDW. The coexistence of the stable node and the stable limit cycle accounts for the hysteresis between pinned and sliding states in this model. However, the limit cycle plays no

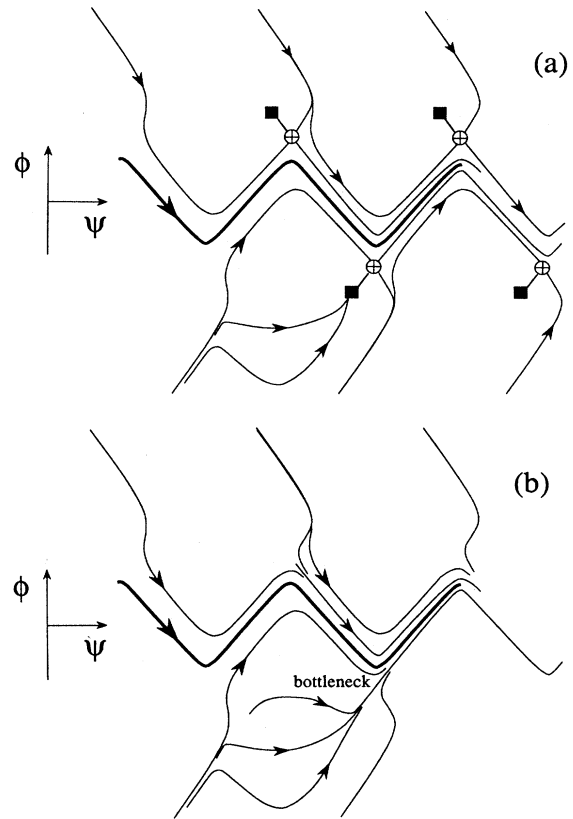


FIG. 4. Phase plane for the screening model Eq. (2). The pictures are  $2\pi$  periodic in the  $\psi$  direction. Parameters:  $\gamma=0.5$ ,  $K=0.05$ , for which  $E_T \approx 0.879528$ . (a) For  $E=0.85 < E_T$ , there is a stable limit cycle (heavy line) and two equilibrium points: a stable node (solid square) and a saddle point (crossed circle). (b) For  $E=0.90 > E_T$ , the saddle and node have coalesced, leaving the limit cycle as the only attractor. Delay occurs when the system passes through the bottleneck before reaching the limit cycle.

part in the depinning transition.

Figure 4(b) shows the phase plane for  $E$  slightly above  $E_T$ . As in the amplitude-collapse model, trajectories are attracted into a bottleneck remnant of the former saddle node. Thus this model also predicts that the time delay scales as  $\varepsilon^{-1/2}$  close to the depinning threshold.

Figure 5 illustrates the delayed onset of the CDW current  $d\psi/dt$  for Eq. (3). The parameters were  $K=0.05$ ,  $\gamma=0.5$ , and  $E=0.88$ . Equation (3) was integrated numerically starting from the zero-field pinned state. For this model and for the parameters chosen, the zero-field pinned state is  $\psi=\pi/2$  and  $\phi\approx 1.43$ . At  $t=0$  the field is turned on. An initial relaxation current is visible in Fig. 5(a) as the system rushes into the bottleneck. Then the system comes to a near standstill. Eventually the system emerges from the bottleneck and the CDW current  $d\psi/dt$  rapidly increases. The system exhibits current oscillations in the sliding state, but for clarity we

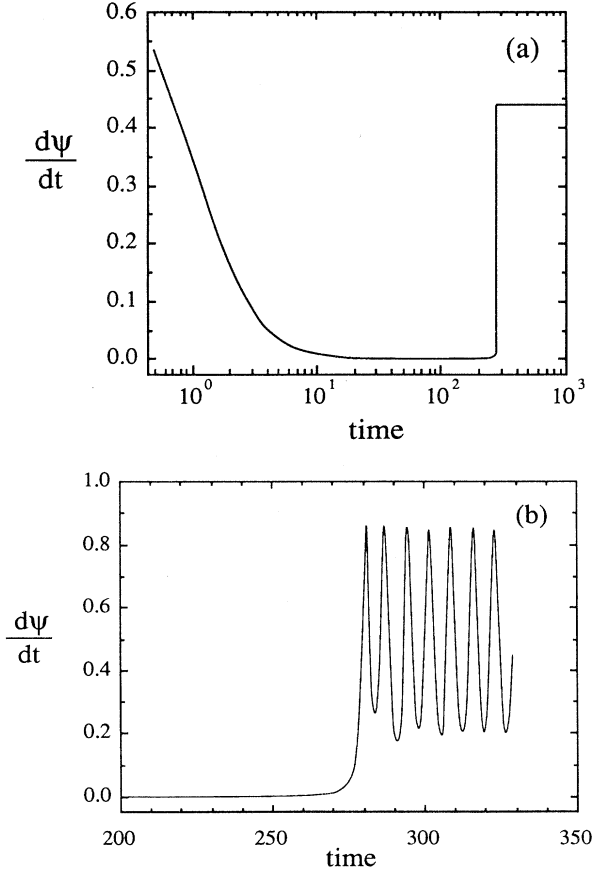


FIG. 5. (a) Delayed onset of the current  $d\psi/dt$  in the screening model Eq. (2). Note that the time axis is logarithmic, and that both time and  $d\psi/dt$  are dimensionless. Curve obtained by numerical integration of Eq. (2) with  $E=0.88$  and other parameters as in Fig. 4. The initial condition was the  $E=0$  pinned state  $\psi=\pi/2$ ,  $\phi=1.4276$ . Current oscillations in the sliding state have been suppressed by time averaging. (b) Same simulation as in (a), but shown at an expanded scale and without time averaging of the oscillations.

have plotted only the mean value of these oscillations in Fig. 5(a).

Figure 5(b) shows the switch and the subsequent current oscillations at an expanded scale. We define the switching delay  $\tau$  by the condition that  $d\psi/dt=0.1$ . Because the switch is rapid any other definition would give essentially the same value for the delay  $\tau$ .

Numerical integration of Eq. (3) confirms the expected square-root scaling of the delay. Figure 6 plots the delay for different values of the normalized overdrive  $\varepsilon$ . The delay scales as  $\varepsilon^{-1/2}$  as  $\varepsilon\rightarrow 0$ . In Fig. 6 this square-root scaling appears to hold over a wider range of  $\varepsilon$  than in the amplitude-collapse model (Fig. 3). A distinctive difference which would allow the two models to be distinguished experimentally is that the screening model yields a  $\tau$  versus  $\varepsilon$  curve which is *concave down*.

### C. Mean-field phase-slip model

In previous papers<sup>19–21</sup> we have presented a mean-field model of CDW transport with phase slip, in which the CDW is regarded as a many-body system of coupled domains. Phase slip due to amplitude collapse between domains is modeled by a periodic coupling term  $\sin(\theta_i - \theta_j)$ , where  $\theta_j$  is the phase of the  $j$ th domain. This coupling force increases approximately linearly for small  $\theta_i - \theta_j$ , then softens and reverses for greater phase differences. The model is closely related to the amplitude-collapse model;<sup>16,17</sup> for example, the sinusoidal coupling is qualitatively similar to the effective phase-phase coupling inherent in the amplitude-collapse model (see Fig. 1 in Ref. 17).

The main simplifying assumption in the model is that the coupling between domains is infinite range. This assumption enables the model to be studied analytically. As we have shown elsewhere,<sup>20,21</sup> the depinning threshold can be calculated exactly, and one can obtain a closed

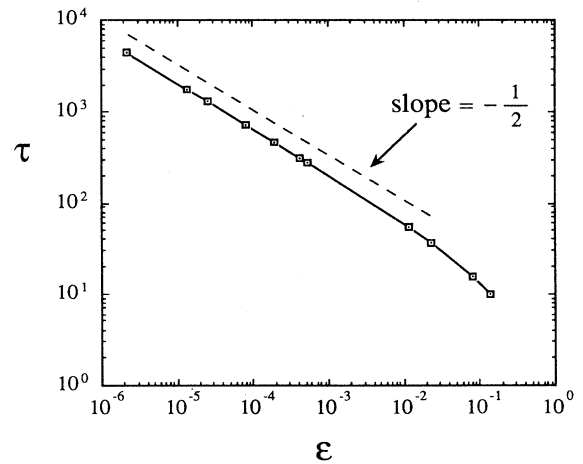


FIG. 6. Dependence of delay  $\tau$  on overdrive  $\varepsilon\equiv(E - E_T)/E_T$ , for the screening model Eq. (2). Curve obtained by numerical integration of Eq. (2), with parameters as in Fig. 4. For small  $\varepsilon$  the curve has a slope of  $-\frac{1}{2}$ , in agreement with bifurcation theory.

form approximation for the switching delay close to threshold. The following treatment is intended as a simplified presentation of some of these results.

The equations for the model are

$$\frac{d\theta_j}{dt} = E + \sin(\alpha_j - \theta_j) + \frac{K}{N} \sum_{i=1}^N \sin(\theta_i - \theta_j),$$

$$j = 1, \dots, N. \quad (4)$$

In Eq. (4),  $\theta_j$  is the phase of the  $j$ th domain,  $E$  is proportional to the applied field,  $K$  is the coupling strength, and  $\alpha_j$  is a random pinning angle between 0 and  $2\pi$ . By an appropriate rescaling of  $E, K$ , and  $t$ , the pinning strength has been normalized to one.

The model is most conveniently analyzed in the limit  $N \rightarrow \infty$ . Then the state of the system is characterized by a function  $\theta_\alpha$  which gives the phase  $\theta$  of the domain with preferred pinning phase  $\alpha$ . The equation of motion becomes

$$\frac{d\theta_\alpha}{dt} = E + \sin(\alpha - \theta_\alpha) + Kr \sin(\psi - \theta_\alpha), \quad \alpha \in [0, 2\pi],$$

$$(5)$$

where we have introduced the complex order parameter  $re^{i\psi}$  defined as

$$re^{i\psi} = \frac{1}{2\pi} \int_0^{2\pi} \exp(i\theta_\alpha) d\alpha.$$

The amplitude  $r$  measures the phase coherence of the system and  $\psi$  is the average phase. The CDW current is taken to be proportional to the rotation rate  $d\psi/dt$  of the order parameter.

The pinned state for the model Eq. (5) is the time-independent solution  $\theta_\alpha = \alpha + \sin^{-1}E$ , for  $\alpha \in [0, 2\pi]$ . This static equilibrium state exists for all  $E \leq 1$  and has coherence  $r = 0$ .

In the amplitude-collapse and screening models considered above, depinning occurs when the pinned state is annihilated in a saddle-node bifurcation. *In the present model the pinned state does not disappear at the depinning threshold—it just loses stability.* To see this, consider the evolution of a small perturbation about the pinned state. Let  $\theta_\alpha = \alpha + \sin^{-1}E + \eta_\alpha$ , where  $\eta_\alpha$  is a small perturbation. Expand  $\eta_\alpha$  as a Fourier series with small amplitudes:

$$\eta_\alpha = \sum_{k=1}^{\infty} a_k \sin k\alpha + \sum_{k=0}^{\infty} b_k \cos k\alpha. \quad (6)$$

Then substituting  $\theta_\alpha$  into Eq. (5) and expanding to first order in the amplitudes, we find that the various modes evolve as follows:

$$\frac{da_1}{dt} = \left[ \frac{K}{2} - (1 - E^2)^{1/2} \right] a_1,$$

$$\frac{db_1}{dt} = \left[ \frac{K}{2} - (1 - E^2)^{1/2} \right] b_1,$$

$$\frac{da_k}{dt} = -(1 - E^2)^{1/2} a_k, \quad k \neq 1$$

$$\frac{db_k}{dt} = -(1 - E^2)^{1/2} b_k, \quad k \neq 1. \quad (7)$$

Equation (7) shows that all the amplitudes decay exponentially fast except  $a_1$  and  $b_1$ , which lose stability when  $K/2 > (1 - E^2)^{1/2}$ . Thus the depinning threshold is given by  $E_T = (1 - K^2/4)^{1/2}$ .

Delayed switching occurs in this model for the same reason as in the first two models: the system is funneled into a bottleneck region of phase space. For this model the static state  $\theta_\alpha = \alpha + \sin^{-1}E$  plays the role of the bottleneck. Systems that are initially incoherent ( $r = 0$ ) evolve toward this bottleneck state because for  $r = 0$ , Eq. (5) reduces to the *uncoupled* system

$$\frac{d\theta_\alpha}{dt} = E + \sin(\alpha - \theta_\alpha). \quad (8)$$

Equation (8) has very simple dynamics: for almost all initial conditions the solutions to Eq. (8) approach the state  $\theta_\alpha = \alpha + \sin^{-1}E$ . A similar behavior occurs for the full system Eq. (5), at least when  $r$  is initially small enough.

In particular, suppose we start the system in the zero-field pinned state, to simulate the experiments where delayed switching is seen. For this model the zero-field pinned state is  $\theta_\alpha = \alpha$ , which has coherence  $r = 0$ . Then we turn on a field  $E > E_T$  at time  $t = 0$ . Because the initial state has coherence  $r = 0$  the system rapidly evolves toward the bottleneck state  $\theta_\alpha = \alpha + \sin^{-1}E$ .

Figure 7 is a schematic representation of the dynamics near the bottleneck. The state space is the space of functions  $\theta_\alpha$ , subject to the periodicity condition  $\theta_0 = \theta_{2\pi} \pmod{2\pi}$ . The origin is the equilibrium state  $\theta_\alpha = \alpha + \sin^{-1}E$ , and the axes correspond to the Fourier amplitudes of the perturbation  $\eta_\alpha$  in Eq. (6). Near the equilibrium state, the linearization Eq. (7) governs the evolution of the amplitudes. Equation (7) shows that at

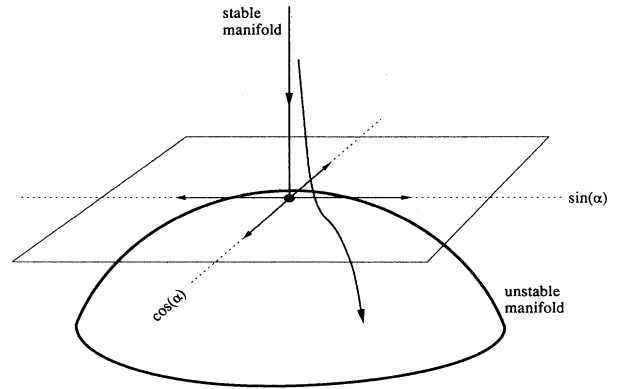


FIG. 7. Schematic plot of the flow in state space for the mean-field phase-slip model Eq. (5). The state space consists of functions  $\theta_\alpha$  that satisfy the periodicity condition  $\theta_0 = \theta_{2\pi} \pmod{2\pi}$ . The origin is the state  $\theta_\alpha = \alpha + \sin^{-1}E$ , which is a saddle point for the flow. The saddle has a two-dimensional unstable manifold whose tangent plane at the origin is spanned by the functions  $\sin(\alpha)$  and  $\cos(\alpha)$ . If the initial state lies close to the stable manifold, then the flow drives it rapidly onto the unstable manifold. From there the state drifts very slowly away from the saddle point and eventually jumps to a distant limit cycle (not shown) corresponding to the sliding state.

the depinning threshold, the state  $\theta_\alpha = \alpha + \sin^{-1}E$  changes from a stable node to a saddle point with two equally unstable directions. These directions correspond to the  $k=1$  modes  $\sin(\alpha)$  and  $\cos(\alpha)$ , as shown in Fig. 7. Thus the unstable manifold<sup>30</sup> of the saddle point is a surface which is tangent to the plane spanned by  $\sin(\alpha)$  and  $\cos(\alpha)$ .

States close to the saddle point are driven rapidly onto the unstable manifold; from there they evolve slowly along the manifold, eventually leaving the neighborhood of the saddle point. When the system has moved sufficiently far from the saddle point, the linear approximation Eq. (7) is no longer adequate, and higher-order terms in the amplitudes must be considered. When the higher-order terms become comparable to the linear terms, the system switches abruptly to a coherent sliding state.<sup>20,21</sup>

Thus the switching delay for Eq. (5) is a sum of three contributions: a rapid approach to the saddle point, a slow evolution along the unstable manifold, and a rapid switch to the sliding state. Near threshold, almost all of the delay is due to the time spent lingering near the saddle. Equation (7) governs the time required to leave the neighborhood of the saddle point. Above threshold, the amplitudes  $a_1$  and  $b_1$  grow approximately exponentially with a time constant  $[K/2 - (1 - E^2)^{1/2}]^{-1}$ . For  $E$  close to  $E_T$ , this time constant scales as  $(E - E_T)^{-1}$  and hence

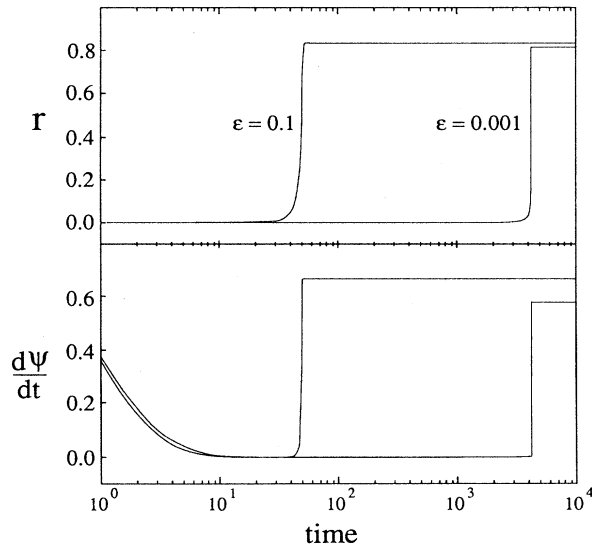


FIG. 8. Delayed onset of the coherence  $r$  and the current  $d\psi/dt$  in the mean-field phase-slip model, for two values of the overdrive  $\epsilon$ . Note that the time axis is logarithmic, and that all quantities shown are dimensionless. Curves are from numerical integration of Eq. (4) with  $N=300$  and  $K=1$ . The initial state was the  $E=0$  pinned state with a small amount of random jitter:  $\theta_j = \alpha_j + \eta_j$ , where  $\eta_j \sim \mathcal{O}(10^{-2})$ . The current  $d\psi/dt$  is large for  $t < 10$  as the system rushes onto the unstable manifold of the saddle point (Fig. 7). Note that for a given  $\epsilon$ , the coherence  $r$  and the current  $d\psi/dt$  switch at the same time. The switching delay increases as  $\epsilon$  tends to zero.

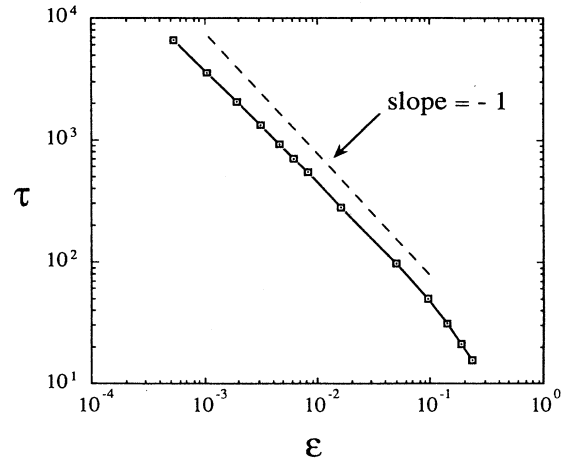


FIG. 9. Dependence of delay on overdrive for the mean-field phase-slip model. Curve obtained by numerical integration of Eq. (4), with parameters as in Fig. 8. For small  $\epsilon$  the curve has a slope of  $-0.93$ , close to the value of  $-1$  predicted by the linear approximation Eq. (7). A nonlinear analysis presented elsewhere (Ref. 21) yields a theoretical curve which accurately matches the numerical data.

as  $\epsilon^{-1}$ . Therefore the switching delay  $\tau$  should scale as  $\epsilon^{-1}$ .

Figures 8 and 9 show that this simple analysis agrees with numerical integration of Eq. (4). Figure 8 shows the evolution of the coherence  $r$  and the CDW current  $d\psi/dt$  for two different values of the overdrive  $\epsilon$ . Note that the jumps in coherence and current occurs simultaneously. Here the switching delay  $\tau$  is defined as the time taken for  $r$  to grow to a value of 0.75.

Figure 9 shows that close to threshold the delay scales approximately as  $\epsilon^{-1}$ . By including nonlinear terms in Eq. (7), we have shown elsewhere<sup>21</sup> that there is a logarithmic correction to this  $\epsilon^{-1}$  scaling. The effect of the logarithmic correction is to cause the effective exponent to be slightly less than 1 (typically between 0.9 and 1). For example, the curve in Fig. 9 has a slope of  $-0.93$  for small  $\epsilon$ . Note also that the curve is slightly concave down over a wide range of  $\epsilon$ .

### III. DISCUSSION

In this paper we have analyzed the dynamics of switching delay in three recent models of CDW transport. The analysis of Sec. II shows that for both the amplitude-collapse model (Sec. II A) and the screening model (Sec. II B), the depinning transition occurs by a saddle-node coalescence. From one point of view this is not surprising—the saddle-node bifurcation is *generic* for dynamical systems with one control parameter (here, the applied electric field). As stated more precisely in Ref. 30, p. 149, “all bifurcations of one-parameter families at an equilibrium with a zero eigenvalue can be perturbed to saddle-node bifurcations.” Thus, for other nonlinear dynamical models of switching, one would generally expect a saddle-node bifurcation at the depinning threshold,

and hence a power-law scaling of the form  $\tau \sim \varepsilon^{-1/2}$  as  $\varepsilon \rightarrow 0$ .

In the mean-field phase-slip model (Sec. II C) the bifurcation is *nongeneric* because of a rotational symmetry in the model: there is no preferred phase  $\psi$  of the complex order parameter. One consequence of this rotational symmetry is that at the depinning transition, the pinned state coalesces simultaneously with an entire *circle* of saddle points.<sup>20</sup> This symmetry also accounts for the simultaneous loss of stability of the  $a_1$  and  $b_1$  modes in Eq. (7) at the depinning threshold.

For the mean-field phase-slip model, the switching delay is predicted to scale as  $\tau \sim \varepsilon^{-1}$ ; a related  $\varepsilon^{-1}$  scaling occurs in systems where a pitchfork bifurcation gives rise to type-III intermittency.<sup>31,32</sup> As with other mean-field theories, e.g., infinite-range models<sup>4,5</sup> of smoothly depinning CDW's, one expects the picture presented here to be qualitatively correct, but possibly with a somewhat different exponent. The mean-field theory of Sec. II C assumes that the coupling between CDW domains is infinite range, whereas the coupling between real CDW domains has a finite range. It is an open problem to determine how the predicted power law  $\tau \sim \varepsilon^{-1}$  would change if the range of the coupling were made finite.

In our analysis we have not discussed one of the leading models of switching, the avalanche-depinning model proposed by Joos and Murray.<sup>15</sup> This model is a variant of the kinetic Ising model, and cannot be analyzed by the bifurcation methods used here. In particular we do not know what this model would predict for the dependence of  $\tau$  on  $\varepsilon$ . This question could be addressed by computer simulation. The model<sup>15</sup> has one realistic feature not shared by the models considered above: for a given applied field  $E$  it predicts a *distribution* of delays, rather than a deterministic dependence of  $\tau$  on  $E$ . The

avalanche-depinning model was motivated by the earlier experiments of Zettl and Grüner,<sup>7</sup> who reported a scatter in the switching delays.

Experiments on switching CDW's are needed to determine how the switching delay  $\tau$  scales with the overdrive  $\varepsilon$ . To our knowledge, two published studies report data relevant to this issue. Kriza *et al.*<sup>8</sup> studied delayed switching in pure and electron-irradiated *o*-TaS<sub>3</sub>. They reported that switching delay increases as threshold is approached, and proposed a phenomenological model which gave good agreement with their data. Their model predicts  $\tau \sim \exp(-\varepsilon)$  close to threshold. Maeda *et al.*<sup>9</sup> studied the field and temperature dependence of switching delay in the blue bronze K<sub>0.3</sub>MoO<sub>3</sub>. For measurements close to threshold ( $\varepsilon < 10^{-1}$ ) their data are consistent with  $\tau \sim \varepsilon^{-1}$  but not with  $\tau \sim \varepsilon^{-1/2}$ .

For all of the models considered here, the predicted scaling laws are robust—they are independent of the values of the microscopic coupling constants, pinning strengths, and other phenomenological parameters. For instance the amplitude-collapse and screening models *always* predict  $\tau \sim \varepsilon^{-1/2}$  as  $\varepsilon \rightarrow 0$ . Because of this robustness, the  $\tau$  versus  $\varepsilon$  dependence should provide a useful experimental benchmark for comparing models based on fundamentally different mechanisms.

#### ACKNOWLEDGMENTS

We thank C. M. Marcus for very stimulating discussions. The research of one of us (S.H.S.) was supported in part by the National Science Foundation, DMS-8605761. This research was supported in part by Office of Naval Research Contract No. N00014-89-J-1023 and N00014-89-J-1592.

\*Present address: Department of Mathematics, 2-380, Massachusetts Institute of Technology, Cambridge, Massachusetts 02139.

<sup>1</sup>*Charge Density Waves in Solids*, Vol. 217 of *Lecture Notes in Physics*, edited by G. Hutiray and J. Solyom (Springer-Verlag, Berlin, 1985).

<sup>2</sup>For a recent review of charge-density-wave dynamics see G. Grüner, *Rev. Mod. Phys.* **60**, 1129 (1988).

<sup>3</sup>H. Fukuyama and P. A. Lee, *Phys. Rev. B* **17**, 535 (1978); P. A. Lee and T. M. Rice, *ibid.* **19**, 3970 (1979); L. Sneddon, M. C. Cross, and D. S. Fisher, *Phys. Rev. Lett.* **49**, 292 (1982); P. B. Littlewood and C. M. Varma, *Phys. Rev. B* **36**, 480 (1987).

<sup>4</sup>L. Sneddon, *Phys. Rev. B* **30**, 2974 (1984).

<sup>5</sup>D. S. Fisher, *Phys. Rev. Lett.* **50**, 1486 (1983); *Phys. Rev. B* **31**, 1396 (1985).

<sup>6</sup>G. Grüner, A. Zawadowski, and P. M. Chaikin, *Phys. Rev. Lett.* **46**, 511 (1981).

<sup>7</sup>A. Zettl and G. Grüner, *Phys. Rev. B* **26**, 2298 (1982).

<sup>8</sup>G. Kriza, A. Jánossy, and G. Mihály, in *Charge Density Waves in Solids*, Ref. 1, p. 426.

<sup>9</sup>A. Maeda, T. Furuyama, and S. Tanaka, *Solid State Commun.* **55**, 951 (1985). Note that in this paper the graph for Fig. 5 is incorrectly printed as Fig. 3.

<sup>10</sup>J. Dumas, C. Schlenker, J. Marcus, and R. Buder, *Phys. Rev. Lett.* **50**, 757 (1983); H. Mutka, S. Bouffard, J. Dumas, and C. Schlenker, *J. Phys. (Paris) Lett.* **45**, L729 (1984); S. Bouffard, M. Sanquer, H. Mutka, J. Dumas, and C. Schlenker, in *Charge Density Waves in Solids*, Ref. 1, p. 449.

<sup>11</sup>K. Svoboda, A. Zettl, and M. S. Sherwin (unpublished).

<sup>12</sup>R. P. Hall, M. F. Hundley, and A. Zettl, *Phys. Rev. Lett.* **56**, 2399 (1986).

<sup>13</sup>R. P. Hall, M. F. Hundley, and A. Zettl, *Phys. Rev. B* **38**, 13 002 (1988); R. P. Hall and A. Zettl, *ibid.* **38**, 13 019 (1988); M. S. Sherwin, A. Zettl, and R. P. Hall, *ibid.* **38**, 13 028 (1988).

<sup>14</sup>M. F. Hundley and A. Zettl, *Phys. Rev. B* **37**, 8817 (1988).

<sup>15</sup>B. Joos and D. Murray, *Phys. Rev. B* **29**, 1094 (1984).

<sup>16</sup>R. P. Hall, M. F. Hundley, and A. Zettl, *Physica B+C* **143B**, 152 (1986).

<sup>17</sup>M. Inui, R. P. Hall, S. Doniach, and A. Zettl, *Phys. Rev. B* **38**, 13 047 (1988).

<sup>18</sup>L. Mihály, Ting Chen, and G. Grüner, *Solid State Commun.* **61**, 751 (1987).

<sup>19</sup>S. H. Strogatz, C. M. Marcus, R. M. Westervelt, and R. E. Mirolo, *Phys. Rev. Lett.* **61**, 2380 (1988).

<sup>20</sup>S. H. Strogatz, C. M. Marcus, R. M. Westervelt, and R. E.

- Mirollo, *Physica D* **36**, 23 (1989).
- <sup>21</sup>C. M. Marcus, S. H. Strogatz, and R. M. Westervelt, *Phys. Rev. B* **40**, 5588 (1989).
- <sup>22</sup>G. Mihály, G. Kriza, and A. Jánossy, *Phys. Rev. B* **30**, 3578 (1984).
- <sup>23</sup>A. Jánossy, G. Mihály, and L. Mihály, in *Charge Density Waves in Solids*, Ref. 1, p. 412.
- <sup>24</sup>P. Chandra, *Phys. Rev. A* **39**, 3672 (1989); D. B. McWhan, G. Aeppli, J. P. Remeika, and S. Nelson, *J. Phys. C* **18**, 1307 (1985).
- <sup>25</sup>F. M. Gardner, *IEEE Trans. Commun. COM-25*, 1210 (1977).
- <sup>26</sup>J. Rinzel and S. M. Baer, *Biophys. J.* **54**, 551 (1988); E. Jakobsson and R. Guttman, *Biophys. J.* **31**, 293 (1980).
- <sup>27</sup>K. Konnerth and C. Lanza, *Appl. Phys. Lett.* **4**, 120 (1964); J. E. Ripper, *J. Appl. Phys.* **43**, 1762 (1972); C. J. Hwang and J. C. Dymont, *J. Appl. Phys.* **44**, 3240 (1973).
- <sup>28</sup>E. P. Harris, *IEEE Trans. Magn.* **15**, 562 (1979); K. Srinivas and J. C. Biswas, *J. Low Temp. Phys.* **74**, 407 (1989).
- <sup>29</sup>J. Sone, *J. Appl. Phys.* **57**, 5028 (1985).
- <sup>30</sup>J. Guckenheimer and P. Holmes, *Nonlinear Oscillations, Dynamical Systems, and Bifurcations of Vector Fields* (Springer-Verlag, New York, 1983).
- <sup>31</sup>Y. Pomeau and P. Manneville, *Commun. Math. Phys.* **74**, 189 (1980); P. Bergé, Y. Pomeau, and C. Vidal, *Order Within Chaos: Towards a Deterministic Approach to Turbulence* (Wiley, New York, 1984), Chap. IX.
- <sup>32</sup>A. Lahiri and T. Nag, *Phys. Rev. Lett.* **62**, 1933 (1989).